Functional Topography: Multidimensional Scaling and Functional Connectivity in the Brain

K. J. Friston, C. D. Frith, P. Fletcher, P. F. Liddle, and R. S. J. Frackowiak

Wellcome Department of Cognitive Neurology, Institute of Neurology, London, United Kingdom

In neuroimaging, functional mapping usually implies *mapping function into an anatomical space*, for example, using statistical parametric mapping to identify activation foci, or the characterization of distributed changes with spatial modes (eigenimages or principal components) (Friston et al., 1993a). This article is about a complementary approach, namely, *mapping anatomy into a functional space*. We describe a simple variant of multidimensional scaling (principal coordinates analysis; Gower, 1966) that uses functional connectivity as its metric. The scaling transformation maps *anatomy* into a *functional space*. The topography, or proximity relationships, in this space embody the functional connectivity among brain regions. The higher the functional connectivity, the closer the regions. Functional connectivity is defined here as the *correlation between remote neurophysiological events*. The technique represents a descriptive characterization of anatomically distributed changes in the brain that reveals the structure of corticocortical interactions in terms of functional correlations. To illustrate the approach we have analyzed data from normal subjects and schizophrenic patients obtained with PET during the performance of word generation tasks. In particular, we focus on prefrontotemporal integration in normal subjects and show that, in schizophrenia, the left temporal regions and prefrontal cortex evidence abnormal functional connectivity.

This article is about the topography of functional brain spaces and corticocortical interactions. We present a descriptive method for characterizing the interrelationships of cortical areas in terms of functional connectivity. The method employs metric multidimensional scaling with functional connectivity as the metric, or measure, that determines the proximity between cortical areas. The objective is to transform anatomical space so that the distance between cortical areas is directly related to their functional connectivity. This transformation defines a new space whose topography is purely functional in nature.

Functional Connectivity

In the analysis of neuroimaging, time series functional connectivity is defined as the *temporal correlations between spatially remote neurophysiological events* (Friston et al., 1993a). This definition is operational and provides a simple characterization of functional interactions. The alternative is to refer explicitly to effective connectivity (i.e., *the influence one neural system exerts over another*) (Friston et al., 1993b). These sorts of concepts were originated in the analysis of separable spike trains obtained from multiunit electrode recordings (e.g., Gerstein and Perkel, 1969; Gerstein et al., 1989; Aertsen and Preissl 1991; Gochin et al., 1991). In electrophysiology, it is often necessary to remove the confounding effects of stimulus-locked transients (which introduce correlations that are *not* causally mediated by direct neural interactions) in order to reveal the underlying *effective* connectivity. The confounding effect of stimulus-locked transients is less problematic in neuroimaging because the promulgation of dynamics from primary sensory areas onward is mediated by neural connections (usually reciprocal and interconnecting). However, it should be remembered that functional connectivity is not necessarily due to effective connectivity and, where it is, effective influences may be indirect. Because functional connectivity (as defined here) is simply a comment on observed correlations, it cannot be used to infer causal relationships in any rich way; however, it does provide a very useful phenomenological characterization of cortical interactions at any scale.

Clearly, the biological nature of functional connectivity in neuroimaging is different from functional connectivity in electrophysiology. The neural networks that might be identified on the basis of phase-locked interactions (using multiunit electrode recordings) in a particular and transient brain state are not the same as macroscopic systems identified on the basis of correlated blood flow observed with neuroimaging over a variety of brain states. However, in both instances the distributed and coordinated physiological changes can be used to infer something about functional interactions either at the level of neural dynamics and phase-locked cohorts or at the level of hemodynamics and cortical coactivations.

Consider two times-series of K hemodynamic measurements, from voxels i and j in the brain. Let m^i_k denoted the kth measurement from voxel i. The functional connectivity between i and j can be defined as

$$\rho_{ij} = \sum m^i_k \cdot m^j_k, \qquad (1)$$

where the time series have been normalized to zero mean and unit sum of squares (Euclidean normalized, i.e., $\Sigma(m^i_k)^2 = 1$). ρ_{ij} is also known as the scalar or dot product of vectors $\mathbf{m}^i$ and $\mathbf{m}^j$. Patterns of functional connections, or correlations, define distributed brain systems. These systems are identified using principal component analysis (PCA) or singular value decomposition (SVD) of the functional connectivity matrix. The distributed systems that ensue are called *eigenimages* or *spatial modes*, and have been used to characterize the spatiotemporal dynamics of physiological time series from several modalities, including multiunit electrode recordings (Mayer-Kress et al., 1991), EEG (Friedrich et al., 1991), MEG (Fuchs et al., 1992), PET (Friston et al., 1993a), and functional MRI (Friston et al., 1993c).

In the present application, functional connectivity is used in a different way, namely, to constrain the proximity of two cortical areas in some functional space. This application capitalizes on the fact that the functional connectivity between i and j is the same as between j and i. This symmetry means functional connectivity can support a measure of distance in a Euclidean sense (a metric). The space on which this measure is made is constructed using multidimensional scaling.

Multidimensional Scaling

Multidimensional scaling is a descriptive method for representing the structure of a system, on the basis of pairwise measures of similarity or confusability (Torgerson, 1958; Shepard, 1980). The resulting multidimensional spatial configuration of the system's elements embodies (in its proximity re-

lationships) the comparative similarities. The technique was developed primarily in the analysis of perceptual spaces. The proposal that stimuli be modeled by points in space, so that perceived similarity is represented by spatial distances, goes back to the days of Isaac Newton (1704). The implementation of this idea is, however, relatively new (Kruskal, 1964; Gower, 1966; Shepard, 1980). In this article we focus on classical or metric scaling (see Chatfield and Collins, 1980). The input to a scaling analysis is a $(n \times n)$ square symmetric matrix of similarities, and the output is an $(n \times r)$ matrix of coordinates of n point in r dimensions. A typical model underlying classical scaling can be summarized by

$$F_{mon}(\delta_{ij}) \cong d_{ij}$$

$$d_{ij} = \sqrt{\sum (x^i_l - x^j_l)^2}, \quad (2)$$

where $F_{mon}(\cdot)$ is a decreasing monotonic function. δ_{ij} is the measure of similarity between elements i and j. d_{ij} is the distance between them in a Euclidean space. x^i_l is the projection of the ith point onto the lth dimension ($\cong$ means equal, except for unspecified error terms). The points are usually plotted in a subspace of this Euclidean space spanned by the r eigenvectors (of the matrix of dot products of the point locations) with "large" eigenvalues (Carroll and Wish, 1974; Chatfield and Collins, 1980; Shepard, 1980) (see below). The resulting distribution of points in the new r-dimensional subspace will capture, in a parsimonious way, the structure of the comparative similarities.

Multidimensional Scaling with Functional Connectivity

In this section we observe that if the correlation or functional connectivity is used as the measure of similarity between brain regions, then there is a very simple way to compute the distances d_{ij} above to construct a functional (multidimensional scaling) space. The approach is equivalent to a principal coordinates analysis (Gower, 1966) of the imaging time series.

One normally considers K measurements at n voxels as K points in an *n-dimensional* space (n-space). However, there is an entirely equivalent representation of n points in a K-space. The distance between points in this K-space can be used directly as a measurement of d_{ij}. This is the same as using the functional connectivity (ρ_{ij}) as the measure of similarity ($\delta_{ij} = \rho_{ij}$), where the function relating similarity and distance is given by

$$F_{mon}(\rho_{ij}) = d_{ij} = \sqrt{2} \cdot \sqrt{1 - \rho_{ij}}. \quad (3)$$

The points in K-space are simply rotated to reveal the greatest structure using the eigenvectors of the $K \times K$ dot product matrix of their locations. This rotation brings the "principal coordinates" of the distribution into view. The veracity of Equation 3 is demonstrated by noting that orthogonal rotation does not change Euclidean distances, and so

$$d_{ij} = \sqrt{\sum (x^i_l - x^j_l)^2} = \sqrt{\sum (m^i_k - m^j_k)^2}$$
$$= \sqrt{2} \cdot \sqrt{1 - \rho_{ij}}, \quad (4)$$

where m^i_k and x^i_l are the coordinates of the points before and after rotation. This approach to identifying the coordinates x^i_l is called a principal coordinates analysis (Gower, 1966), although the term classical scaling is preferred to avoid confusion with PCA (Chatfield and Collins, 1980).

Although care has been taken to relate this characterization of functional topography to classical scaling, principal coordinates analysis, and metric multidimensional scaling, the underlying idea is very simple: imagine K measures from n voxels plotted as n points in a K-space. Because they have been normalized to zero mean and unit sum of squares, these points will fall on an $K - 1$ dimensional hypersphere. The closer any two points are to each other, then the greater their correlation or functional connectivity (in fact, the correlation is the cosine of the angle subtended at the origin). The distribution of these points embodies the functional topography. A view of this distribution, that reveals the greatest structure, is simply obtained by rotating the points to maximize their apparent dispersion (variance). In other words, one looks at the subspace with the largest "volume" (spanned by the eigenvectors with the largest eigenvalues). Note that in this view (or projection) the distances seen will not be the actual distances in the $K - 1$ dimensional space. One can either regard this discrepancy as being attributable to "noise" (where the variance in the remaining dimensions is sufficiently small to be ignored and the equality in Eq. 3 becomes $\cong$), or acknowledge explicitly that one is looking at a high dimensional space "from the side."

Mathematically, this rotation can be implemented using SVD. Let $\mathbf{M} = [\mathbf{m}^1 \ldots \mathbf{m}^n]$ be a matrix of the normalized data (one column vector per voxel time series), and $\mathbf{X} = [\mathbf{x}^1 \ldots \mathbf{x}^r]^T$ be the matrix of desired coordinates (^{T} denotes transposition). Using SVD, $\mathbf{M}$ can be factorized (Golub and Van Loan, 1991):

$$[\mathbf{usv}] = \mathrm{SVD}\{\mathbf{M}\}$$

such that

$$\mathbf{M} = \mathbf{u} \cdot \mathbf{s} \cdot \mathbf{v}^T, \quad (5)$$

where $\mathbf{u}$ and $\mathbf{v}$ are unitary orthogonal matrices and $\mathbf{s}$ is a diagonal matrix. The principal axes of the n points in K-space are given by the eigenvectors of $\mathbf{M} \cdot \mathbf{M}^T$, that is, $\mathbf{u}$:

$$\mathbf{M} \cdot \mathbf{M}^T = \mathbf{u} \cdot \lambda \cdot \mathbf{u}^T,$$

where $\lambda = \mathbf{s}^2$ and

$$\mathbf{X} = \mathbf{M}^T \cdot \mathbf{u}. \quad (6)$$

Voxels that have a correlation of unity will occupy the same point in the new space. Voxels that have independent dynamics ($\rho_{ij} = 0$) will be $\sqrt{2}$ apart. Voxels that are negatively but totally correlated ($\rho_{ij} = -1$) will be maximally separated (by a distance of 2). Profound negative correlations denote a functional association that are modeled in the functional space as diametrically opposed locations on the hypersphere. In other words, two regions with profound negative correlations will form two "poles" in functional space.

There is an interesting aspect of this application of classical scaling to neuroimaging data. Normally, the data used in multidimensional scaling represent similarities between discrete elements (e.g., voxels). However, neuroimaging data can also be thought of as a good lattice representation of a continuous and smooth process in anatomical space. This means that the scaling transformation represents a mapping (or distortion) of one volume into another. In other words an anatomical region (e.g., the superior temporal gyrus) has a continuous and distributed representation in the functional space defined by the scaling procedure. The location and shape of this new volume will, of course, be completely different from the anatomical volume, but local contiguity relationships will be preserved. This preservation is due to high local autocorrelations (smoothness) in the underlying process (that is assumed to have a twice differentiable autocorrelation function at zero). Consider two points in the image process separated by $\mathbf{dx}$. As $\mathbf{dx}$ tends to zero the correlation between the two points will tend to unity (because of the assumption about the autocorrelation function) and the distance in functional space will tend to zero by Equation 3. In other words, prox-

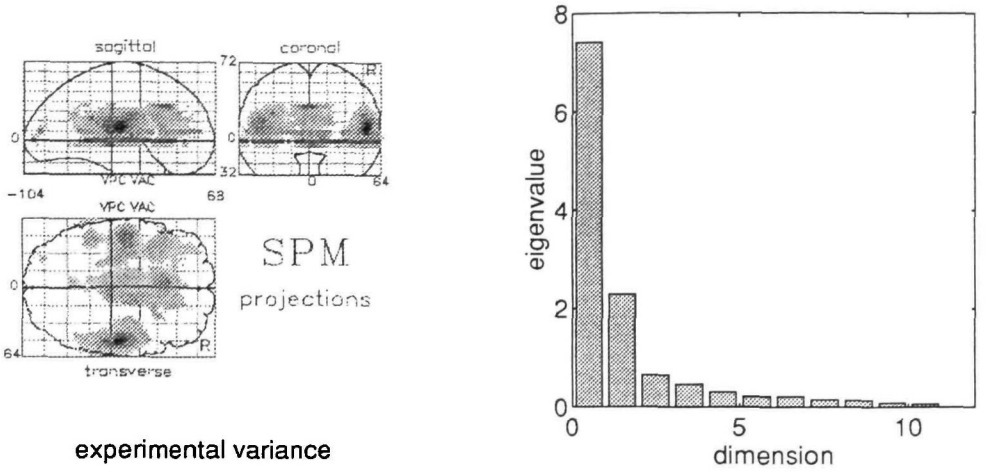

Figure 1. Experimentally introduced variance. *Left,* Statistical parametric map (*SPM*) of the *F* ratio following an ANCOVA of the six-subject, 12-condition verbal fluency study. The display format is standard and provides three views of the brain in the stereotactic space of Talairach and Tournoux (1988) (from the back, from the right, and from the top). *Right,* Eigenvalues (singular values squared) of the functional connectivity matrix reflecting the relative amounts of variance accounted for by the 11 dimensions of the functional space. Only two eigenvalues are greater than unity and to all intents and purposes the space defined by classical scaling can be considered two dimensional.

imate points in anatomical and functional spaces both tend to zero in the limit of small separations. Contiguity of this sort implies that bounded regions in anatomical space remain connected in functional space (however tenuously); however, these regions may be intersect themselves in a highly complicated way and two anatomical regions can occupy the same functional space. Clearly for real (voxel) data this contiguity preservation depends on voxel sizes being "small" relative to the width of the autocorrelation function. For PET data this is assured but in other modalities (e.g., functional MRI) this may not be the case.

In what follows, anatomical regions are represented as continuous distributions in functional space with varying density. This density is simply the density of points corresponding to voxels in the original anatomical volume.

The Functional Topography of Word Generation

In this section we apply the scaling transformation to a PET time series from a verbal fluency activation study. These data are the same used to illustrate the identification of spatial modes using PCA in Friston et al. (1993a). In brief, the data were obtained from six subjects scanned 12 times (every 8 min) while performing one of two verbal tasks. Scans were obtained with a CTI PET camera (model 953B, CTI, Knoxville, TN). ^{15}O was administered intravenously as radiolabeled water infused over 2 min. Total counts per voxel during the buildup phase of radioactivity served as an estimate of regional cerebral blood flow (rCBF) (Fox and Mintun, 1989). Subjects performed two tasks in alternation. The first task involved repeating a letter presented aurally at one per 2 sec (*word shadowing*). The second was a paced verbal fluency task, where the subjects responded with a word that began with the letter presented (*intrinsic word generation*). To facilitate intersubject pooling, data were stereotactically normalized (Friston et al., 1990) and whole brain differences were removed using ANCOVA (Friston et al., 1991). Although the scaling transformation can be applied to single subjects, we used the average voxel rCBF over all the subjects for the same reasons given in Friston et al. (1993a).

A subset of voxels was selected in which a significant amount of variance, due to the 12 conditions, was observed [ANCOVA $F(11,54) > 2.6, p < 0.05$]. This subset is shown in a statistical parametric map (Friston et al., 1991) of the *F* ratio in Figure 1 (left). The time series from each of these voxels formed the data matrix **M** with 12 rows (one for each condition) and 6477 columns (one for each voxel). Following normalization (to zero mean and unit sum of squares over each column), **M** was subject to singular value decomposition according to Equation 5 and the coordinates **X** of the voxels in the functional space computed as in Equation 6.

This space was essentially two dimensional (only two eigenvalues were greater than unity; see Fig. 1, right). The location of voxels in this two-dimensional subspace is shown in Figure 2 by rendering voxels from different regions in different colors. The anatomical regions corresponding to the different colors are shown in the top row. Anatomical regions were selected to include those parts of the brain that showed the greatest variance during the 12 conditions (Fig. 1, left). Anterior regions (Fig. 2, right) included the mediodorsal thalamus (blue), the dorsolateral prefrontal cortex (DLPFC) and Broca's area (red), and the anterior cingulate (green). Posterior regions (Fig. 2, left) included the superior temporal regions (red), the posterior superior temporal regions (blue), and the posterior cingulate (green). The voxels constituting these regions were within 20 mm of appropriate centers selected from the atlas of Talairach and Tournoux (1988) (see Table 1). The reason that anterior and posterior regions are presented separately is simply due to the fact that there are only three primary colors to play with, but there are more than three regions of interest.

The corresponding functional space (Fig. 2, lower row) reveals a number of things about the functional topography elicited by this set of activation tasks. First, each anatomical region maps into a relatively localized portion of functional space. This preservation of local contiguity reflects the high correlations within anatomical regions, due, in part, to smoothness in the original data and to high degrees of intraregional functional connectivity. Second, the anterior regions are almost in juxtaposition, as are the posterior regions; however, the confluence of anterior and posterior regions form two diametrically opposing poles (or one axis). This configuration suggests an anterior-posterior axis with prefrontotemporal and cingulocingulate components. Third, within the anterior and posterior sets of regions certain generic features are evident. The most striking is particular ordering of functional interactions. For example, the functional connectivity between the posterior cingulate (green) and superior temporal regions (red) is high and similarly for the superior temporal (red) and posterior temporal regions (blue), yet the posterior cingulate and posterior temporal regions show very little functional connectivity (they are $\sqrt{2}$ apart or equivalently subtend 90° at the origin). Finally, within the main anteroposterior axis there appear to be two subordinate axes. The first is a prefrontotemporal axis (red/blue-red), and the second is an anterior-posterior cingulate axis (green-green). These two axes are closely aligned but are not completely confounded.

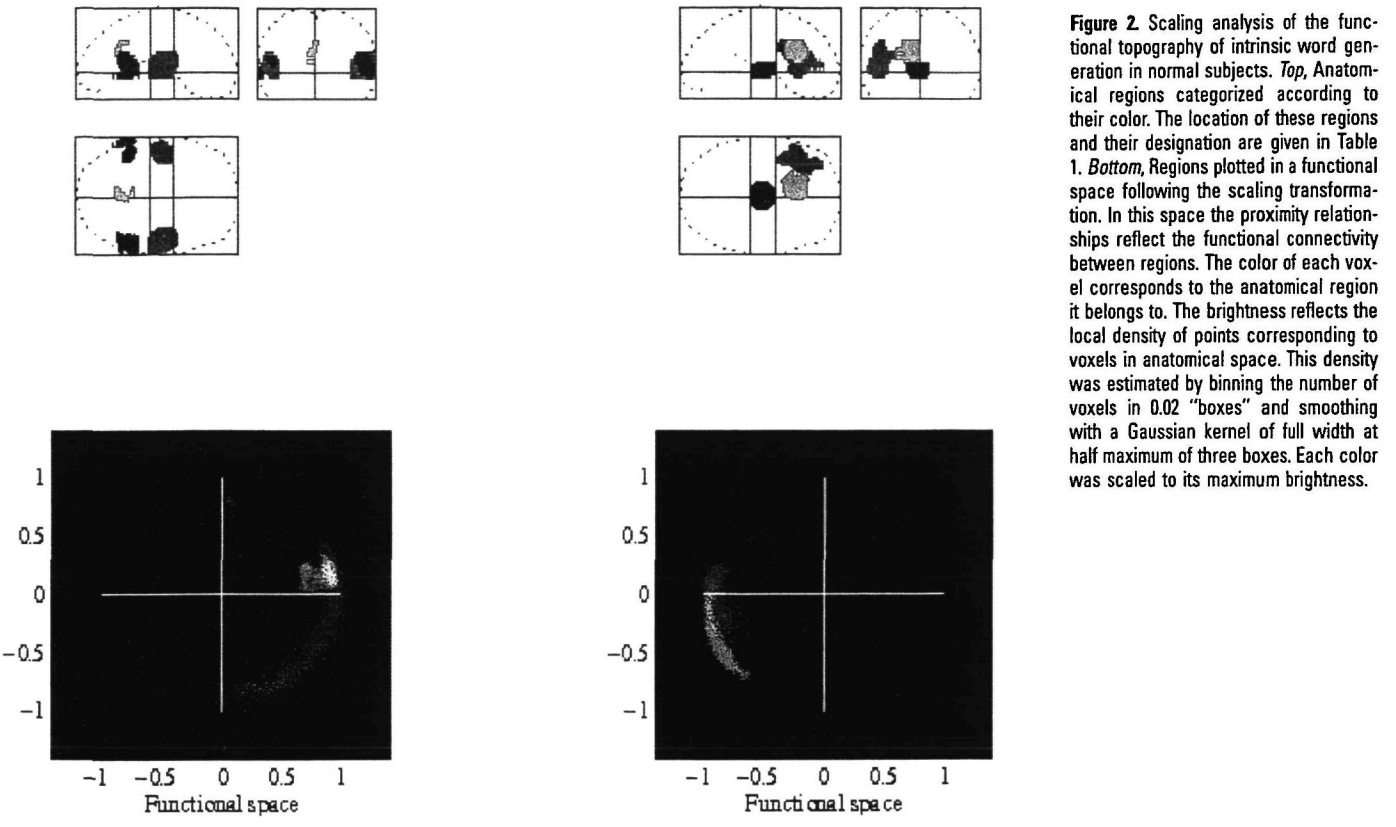

Figure 2. Scaling analysis of the functional topography of intrinsic word generation in normal subjects. *Top,* Anatomical regions categorized according to their color. The location of these regions and their designation are given in Table 1. *Bottom,* Regions plotted in a functional space following the scaling transformation. In this space the proximity relationships reflect the functional connectivity between regions. The color of each voxel corresponds to the anatomical region it belongs to. The brightness reflects the local density of points corresponding to voxels in anatomical space. This density was estimated by binning the number of voxels in 0.02 "boxes" and smoothing with a Gaussian kernel of full width at half maximum of three boxes. Each color was scaled to its maximum brightness.

These results are consistent with known anatomical connections. For example, DLPFC–anterior cingulate connections, DLPFC–temporal connections, bitemporal commissural connections, and mediodorsal thalamic–DLPFC projections have all been demonstrated in nonhuman primates (e.g., Goldman-Rakic, 1986, 1988). The mediodorsal thalamic region and DLPFC are so correlated that one is embedded within the other (purple area). This is pleasing, given the known thalamocortical projections to the DLPFC.

Interpretation of the Functional Space

At this point, one might ask if absolute position in this functional space has any meaning. For example, is the fact that the prefrontotemporal axis is horizontal (as opposed to vertical) important. The answer is yes. The dimensions of the transformed space have specific functional attributions that depend on the tasks employed to elicit the functional interactions. Because the dimensions of the functional space are defined by unit vectors in a *K*-space of tasks, *each dimension is associated with a particular profile of the experimental conditions.* For example, the first dimension points in the direction of all the intrinsic word generation tasks and away from the baseline word-shadowing tasks. Conversely, the second dimension points toward the first scans and away from the last scans. The vectors defining these directions are simply the first two columns of **u** and are shown in Figure 3 (left). On the basis of these task-dependent profiles one could designate the first dimension of the functional space as *intentional* (corresponding to the intentional or intrinsic generation of words) and the second as *attentional* (attentional changes or changes in perceptual set as the experiment proceeds).

This perspective provides a slightly richer interpretation of the functional space in the following way: functional connectivity (distance) between two regions can be partitioned into intentional (horizontal) and attentional (vertical) components. For example, the horizontal proximity of the DLPFC (red) and anterior cingulate (green) is greater than their vertical proximity. In other words, the functional connectivity between the DLPFC and anterior cingulate is dominated by the intentional aspects of the tasks used to elicit the functional interactions. Similarly, the (horizontal) prefrontotemporal axis is almost entirely intentional, whereas the (oblique) anteroposterior cingulate axis suggests both intentional and attentional components. This interpretation will be important below in examining the functional topography of schizophrenia.

Table 1
Location of anatomical regions in Talairach and Tournoux stereotaxic space

Name	Location x,y,z (mm)	Putative Brodmann's area	Color
Mediodorsal thalamus	0 −12 4		blue
Left DLPFC	−48 32 12	46	red
Broca's area	−58 16 24	44	red
Anterior cingulate	−12 24 24	32	gren
Posterior cingulate	−8 −48 24	32	green
Superior temporal gyrus	±56 8 4	21	red
Posterior middle temporal gyrus	±54 −56 0	22	blue

Regions chosen for the analysis of the 12-condition word generation study of normal subjects. All voxels that reached criteria following ANCOVA and fell within 20 mm of the above location constituted a "region." See Figure 2 (left) for a graphical presentation of this anatomical parcellation.

The Relationship between the Functional Space and the Spatial Modes (Eigenimages) of the Time Series

The last part of this section comments on the intimate relationship between the dimensions of the functional space and the eigenimages or spatial modes associated with the time

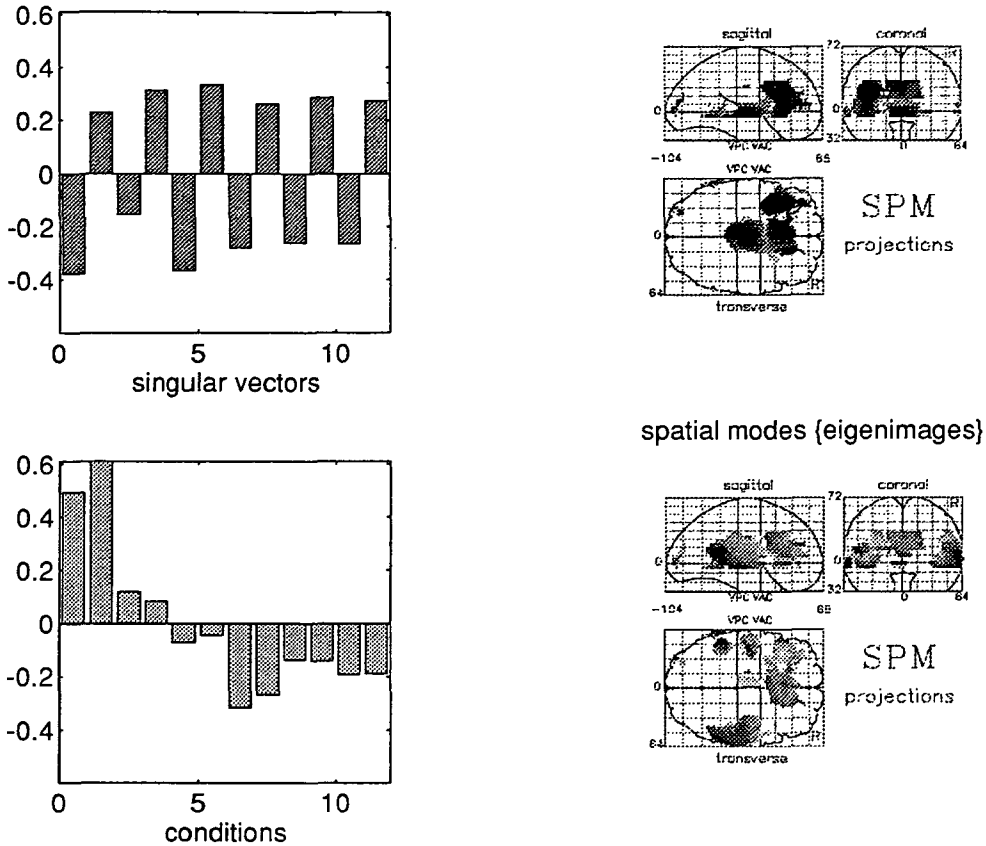

Figure 3. Functional attribution of the functional space. *Left,* Eigenvectors of the distribution of points in the functional space, for instance, eigenvectors of $\mathbf{MM}^T$. These eigenvectors (or singular vectors) are unit vectors that define a direction in functional space. The attribution of this direction or dimension depends on relating this vector to the tasks employed during the activation. The first eigenvector (*top*) is clearly related to the difference between word generation (even-numbered conditions) and word shadowing (odd-numbered scans). This difference is the intentional or intrinsic generation of word representations. The second eigenvector (*bottom*) corresponds to some largely monotonic time effect we have labeled attentional. *Right,* The eigenimages corresponding to the first two eigenvectors of the functional connectivity matrix. These eigenimages (or spatial modes) are the eigenvectors of $\mathbf{M}^T\mathbf{M}$. The eigenimages are displayed as a maximum intensity projection in standard SPM format. The color scale is arbitrary, and each SPM is scaled to its maximum.

series. The relationship is, in fact, very simple (see Chatfield and Collins, 1980, p. 200). The time-dependent expression of the eigenimages are the same as the vectors describing the dimensions in the functional *K*-space. Figure 3 (right) show the eigenimages that correspond to the two dimensions used in the scaling transformation. They are images of the first two columns of $\mathbf{v}$ in Equation 5 (see Friston et al., 1993a, for a fuller discussion of how one interprets these eigenimages). In brief, they represent the distributed systems that best account for the observed variance-covariance structure exhibited by a neurophysiological time series (it should be noted that the eigenimages presented here are not exactly the same as those presented in Friston et al. (1993a), because the current eigenimages are images of the eigenvectors of the correlation matrix, as opposed to the covariance matrix that is usually used). Consider again the singular value decomposition of $\mathbf{M}$:

$$\mathbf{M} = \mathbf{u}\cdot\mathbf{s}\cdot\mathbf{v}^T$$

and

$$\mathbf{M}^T\mathbf{M} = \rho = \mathbf{v}\cdot\lambda\cdot\mathbf{v}^T.$$

Therefore, $\mathbf{v}$ is a matrix whose columns correspond to the eigenimages of $\mathbf{M}$. The rotation implicit in our scaling approach is effected by

$$\mathbf{X} = \mathbf{M}^T\cdot\mathbf{u} = \mathbf{v}\cdot\mathbf{s}.$$

$\mathbf{X}$ is a matrix of the eigenvectors $\mathbf{v}$ scaled by their singular values. Put simply, one can either use the eigenvectors of the functional connectivity matrix to (1) generate a series of eigenimages, or (2) scale them according to their singular values and use them as coordinates to construct a functional space. These two analyses (principal coordinates analysis and principal components analysis) are entirely equivalent from a mathematical point of view, but reveal the nature of functional interactions from different perspectives.

Functional Disintegration in Schizophrenia

In this section we present an analysis of previously published PET data examining functional connectivity in schizophrenia (Friston et al., 1996). The notion that schizophrenia represents a disintegration of the psyche is as old as its name, introduced by Bleuler (1913) to convey a "splitting" of mental faculties. We have investigated the hypothesis that this mentalistic "splitting" has a physiological basis, with a precise and regionally specific character.

Neurodevelopmental (e.g., Weinberger, 1987) and cognitive models of schizophrenia (e.g., Frith, 1987) have emphasized abnormal frontolimbic and prefrontotemporal integration. Structural MRI studies of schizophrenic brains have found abnormalities in the temporal cortex and underlying white matter with some consistency (Shenton et al., 1992; Williamson et al., 1992; McCarley et al., 1993). Our previous analysis of the eigenimages, derived from word-generation PET activation studies, in normal subjects and schizophrenic patients, pointed to abnormal functional connectivity between the left dorsolateral prefrontal cortex (DLPFC) and the left superior and middle temporal gyri (Friston et al., 1996). We applied the scaling transformation to the data in the hope of revealing, in a direct way, the relationship between the temporal regions and prefrontal areas, in terms of functional connectivity.

The details of the experimental design and data acquisition have been described elsewhere (Friston et al., 1996) and will be summarized briefly. Four groups of six subjects were scanned six times during the performance of a series of word-generation tasks (verbal fluency, semantic categorization, and

word shadowing; each task was preformed twice in balanced order). The four groups comprised (1) controls, a normal group; (2) poor, patients who produced a small number of words during FAS verbal fluency; (3) odd, patients who produced odd, inappropriate words; and (4) unimpaired, patients whose performance was near normal. The patients all met DSMIII-R criteria (American Psychiatric Association, 1987) for schizophrenia.

The data were stereotactically normalized (Friston et al., 1991) and a mean rCBF estimate for each voxel, for each condition, for each group, was obtained by averaging over subjects in each group using the same techniques mentioned in the previous section. A subset of voxels was selected at which differences between any of the six scans accounted for a significant amount of variance [ANCOVA, $F(5,24) > 3.9$, $p < 0.001$] in one or more of the four groups. The result was a large matrix of rCBF estimates (**M**), each comprising six rows (one for each condition) and 4802 × 4 columns (one for each voxel in each group). **M** was normalized to a mean of zero and unit sum of squares (over each column).

The matrix (**M**) was subject to the scaling transformation, as described in the above section. Note that all four groups were entered at the same time. This meant that the functional designation of the dimensions of the functional space was the same for all groups. The results of these analyses are seen in Figures 4 and 5. Figure 4 (left) shows the anatomical regions rendered in subsequent figures. They included the left DLPFC and medial prefrontal cortex (red), the left superior temporal region (green), and the left posterior middle temporal cortex (blue). Table 2 gives the centers of these regions in stereotactic coordinates. The two dimensions used in the scaling transformation were very similar to the intentional and attentional dimensions seen in the previous section. The first dimension (Fig. 4, top right) pointed toward the verbal fluency (first and last conditions) and away from word shadowing (middle conditions). It was largely indifferent (orthogonal) to the semantic categorization conditions. The second dimension showed monotonic time effects suggesting physiological adaptation due to putative attentional changes.

The functional space for the normal subjects and the schizophrenic groups are shown in Figure 5. In the normal subjects (top left), this set of tasks elicited a prefrontotemporal axis. The axis is slightly oblique, suggesting some of this functional connectivity is due to systematic time-dependent effects. The similarity between this configuration and that of similar regions in the previous section is evident. The equivalent spaces for the schizophrenic groups are markedly different from the normal space. Although the DLPFC (red) has retained its position, the temporal regions have moved across from the opposite side to occupy a domain that spans high positive correlations with the DLPFC to total independence. The migration of the superior temporal regions is remarkably consistent across the three schizophrenic groups and is predominantly in a right-left direction, suggesting this abnormality is due to intentional aspects of the tasks employed. Conversely, the posterior temporal regions are less consistent in their displacement. The horizontal (intentional) shift is similar in all three groups, but the vertical or attentional component is different for each of the three groups (the unimpaired group showed a pronounced movement of posterior temporal regions in the attentional dimension). This suggests that the functional connectivity elicited by intentional aspects of the word generation tasks result in an abnormal pattern of prefrontotemporal integration that is largely invariant over different schizophrenic subgroups. However, the (dys)functional connectivity elicited by attentional components is specific to the group in question.

Notice that in the *poor* group the distance between the left DLPFC (red) and the superior temporal regions (green) suggests an absence of functional connectivity (positive or negative). This represents a true left prefronto-superior temporal disintegration.

This is not the place to embark on a detailed analysis of these results in terms of the neuropsychology of schizophrenia; however, it is worth pointing out that the observed reversal and/or loss of prefrontotemporal integration is particularly relevant given the signs and experiential symptoms of schizophrenia (for a fuller discussion, see Frith, 1993; Friston et al., 1996).

Discussion

We have presented a simple application of metric multidimensional scaling that uses functional connectivity as the underlying metric. Functional connectivity is simply the correlation between remote neurophysiological events. The technique provides an expedient transformation that maps anatomical space into a functional space. The topography of this functional space is such that proximity implies a high degree of functional connectivity. The nature of this mapping means that anatomically distributed systems that are functionally connected converge toward the same locus in functional space.

Potential applications of the technique have been demonstrated in the context of word generation in normal subjects and abnormal prefrontotemporal integration in schizophrenia. In particular, the negative correlations between prefrontal and temporal activity normally seen are reversed in schizophrenia and the left superior temporal gyrus appears to be dissociated from the prefrontal systems implicated in word generation.

The techniques described here are not new. Principal coordinates analysis or classical metric scaling was introduced in the 1960s, and other forms of multidimensional scaling have been used in the context of neuroimaging (see Goldenberg, 1989; Goldenberg et al., 1989). What is new here is that the correlations used in the classical scaling are correlations in neuroimaging time series. These correlations are a simple characterization of functional interactions and render the space defined by the scaling technique meaningful in terms of functional connectivity. The second novel aspect of the proposed (voxel-based) application is that the transformation can be thought of as being applied to continuous volumes (if the voxel data are a good lattice representation of a smooth continuous processes).

The Relationship between Eigenimages, Spatial Modes, and Functional Topography

There is a pleasing and complementary relationship between functional topography defined using the scaling transformation and the use of the eigenvector solution of the functional connectivity matrix to identify spatial modes (e.g., Friedrich et al., 1991; Friston et al., 1993a). In the latter approach, the data are considered as K points in an n-dimensional space. These points define a trajectory in a space who dimensions are voxels. The principal axes (eigenvectors) of the distribution traced out by the trajectory correspond to the spatial modes embedded within the data. An image of these eigenvectors is called an eigenimage. Eigenimages, or spatial modes represent a simple and powerful way of mapping *function into anatomical space.*

In defining a functional space one considers the data as n points in an K-dimensional space. The principal axes (eigenvectors) of this distribution are used to rotate the points to reveal the greatest structure in their interrelationships. A subspace of the rotated points represents a *mapping of anatomy into a functional space.*

Figure 4. The functional topography of normal subjects and schizophrenic patients. *Left,* Anatomical regions detailed in Table 2. *Right,* The first two eigenvectors of the distribution in the functional space showing that the first (*top*) vector is associated with the difference between the first and last conditions (intrinsic word generations) and the middle two conditions (word shadowing). The second vector (*below*) corresponds to a monotonic time effect.

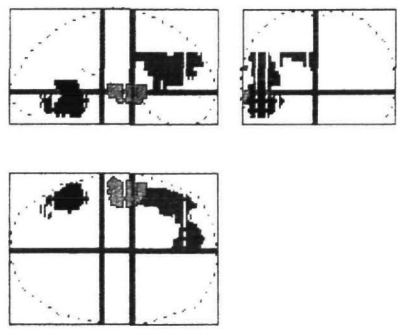

Anatomical regions

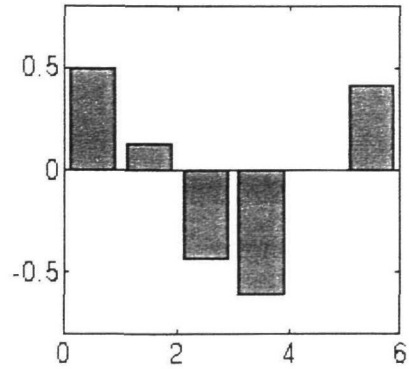

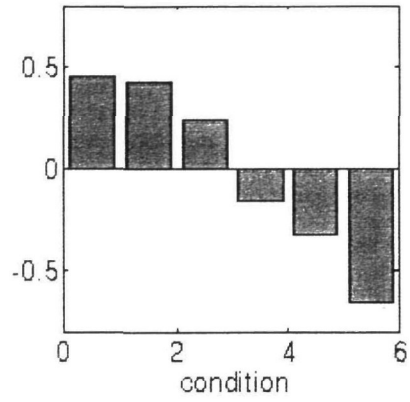

Figure 5. The functional topography of normal subjects and schizophrenic patients. *Top left,* Functional space of the normal group demonstrating the marked prefrontotemporal axis that characterizes normal functional connectivity. *Top right,* The equivalent space for the poor group of schizophrenic subjects in which all the temporal regions have migrated from the left-hand pole to the bottom right quadrant. This corresponds to a loss and reversal of normal negative prefrontotemporal functional connectivity. *Bottom left,* Functional space for the odd group. *Bottom right,* Functional space for the unimpaired group.

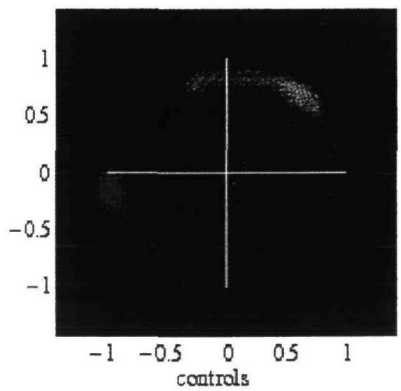

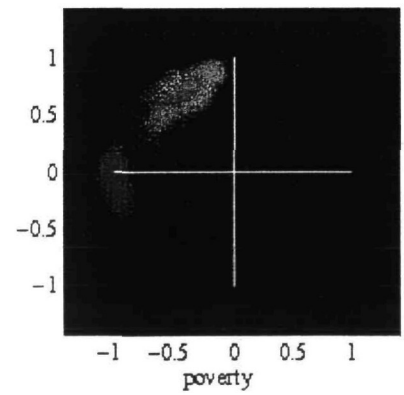

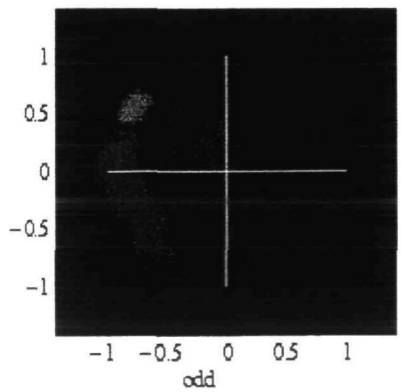

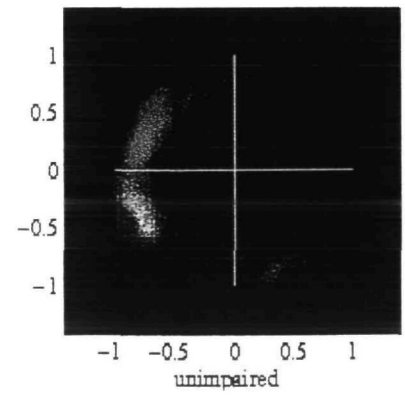

Table 2
Location of anatomical regions in Talairach and Tournous stereotaxic space

Name	Location x,y,z (mm)			Putative Brodmann's area	Color
Left DLPFC	−48	36	12	46	red
Broca's area	−58	16	24	44	red
Medial PFC	−12	46	24	9	red
Superior temporal gyrus	−56	−8	4	22	green
Posterior middle temporal gyrus	−40	−58	−8	21	blue

Regions chosen for the analysis of the six-condition word generation study of normal subjects and schizophrenic patients. All voxels that reached criteria following ANCOVA and fell within 20 mm of the above location constituted a "region." See Figure 4 (left) for a graphical presentation.

As with eigenimages, the functional spaces created using classical scaling will change fundamentally with different brain states and are, as a consequence, experiment and time dependent.

There is a parallel between the present work, using functional connectivity and that of Young (1992) who used a meta-analysis of anatomical connectivity and nonmetric multidimensional scaling. This analysis allowed the authors to comment on the segregation of dorsal and ventral processing streams and reconvergence in the DLPFC and the superior temporal area. Although we have chosen to illustrate the technique with an (important) example of abnormal functional topography in schizophrenia, there are clearly many applications to normal functional anatomy. It would be interesting to examine the issues addressed by Young (1992) to provide a complementary functional perspective. The technique applied in this article uses metric multidimensional scaling as opposed to nonmetric scaling used by Young (1992). There have been some concerns expressed about the application of nonmetric scaling to connectivity data (Simmen et al., 1994; Young et al., 1994). These concerns are avoided with metric scaling. In this sense, the current application of metric scaling could prove very useful in resolving important questions about large scale connectivity and functional organization in the brain.

At the present time, it is not easy to make statistical inferences about the topographic features or changes in these features obtained with multidimensional scaling (Chatfield and Collins, 1980); however, this does not detract from the proposed application as a powerful descriptive approach to neuroimaging data.

Notes

This work was based on an original idea of Stephen Kosslyn. We are indebted to him for his inspirational comments and ensuing persistence. We also thank our colleagues at the MRC Cyclotron Unit, without whom these studies would not have been possible.

Address correspondence to Wellcome Department of Cognitive Neurology, Institute of Neurology, Queen Square, London WC1N 3BG, UK.

References

Aertsen A, Preissl H (1991) Dynamics of activity and connectivity in physiological neuronal networks. In: Non linear dynamics and neuronal networks, pp 281–302. New York: Schuster.

American Psychiatric Association (1987) Diagnostic and statistical manual of mental disorders, 3d ed, rev. Washington, DC: American Psychiatric Press.

Bleuler E (1913) Dementia praecox or the group of schizophrenias (Engl trans). In: The clinical routes of the schizophrenia concept (Cutting J, Shepherd M, eds). Cambridge: Cambridge UP, 1987.

Carroll JD, Wish M (1974) Models and methods for three-way multidimensional scaling. In: Contemporary developments in mathematical psychology, Vol 1 (Atkinson RC, Krantz DH, Luce RD, Suppes P, eds), pp 57–88. San Francisco: Freeman.

Chatfield C, Collins AJ (1980) Introduction to multivariate analysis, pp 189–210. London: Chapman and Hall.

Fox PT, Mintun MA (1989) Non-invasive functional brain mapping by change distribution analysis of averaged PET images of $H^{15}O_2$ tissue activity. J Nucl Med 30:141–149.

Friedrich R, Fuchs A, Haken H (1991) Modelling of spatio-temporal EEG patterns. In: Mathematical approaches to brain functioning diagnostics (Dvorak I, Holden AV, eds). New York: Manchester UP.

Friston KJ, Frith CD, Liddle PF, Dolan RJ, Lammertsma AA, Frackowiak RSJ (1990) The relationship between global and local changes in PET scans. J Cereb Blood Flow Metab 10:458–466.

Friston KJ, Frith CD, Liddle PF, Frackowiak RSJ (1991) Plastic transformation of PET images. J Comput Assist Tomogr 15:634–639.

Friston KJ, Frith CD, Liddle PF, Frackowiak RSJ (1993a) Functional connectivity: the principal component analysis of large (PET) data sets. J Cereb Blood Flow Metab 13:5–14.

Friston KJ, Frith CD, Frackowiak RSJ (1993b) Time-dependent changes in effective connectivity measured with PET. Hum Brain Mapping 1:69–80.

Friston KJ, Jezzard P, Frackowiak RSJ, Turner R (1993c) Characterizing focal and distributed physiological changes with MRI and PET. In: Functional MRI of the brain, pp 207–216. Berkeley, CA: Society of Magnetic Resonance in Medicine.

Friston KJ, Herold S, Fletcher P, Silbersweig D, Cahill C, Dolan RJ, Liddle PF, Frackowiak RSJ, Frith CD (1996) Abnormal fronto-temporal interactions in schizophrenia. In: ARNMD series, Vol 73, Biology of schizophrenia and affective disease (Watson SJ, ed), pp 421–449. Washington, DC: ARNMD.

Frith CD (1987) The positive and negative symptoms of schizophrenia reflect impairments in the initiation and perception of action. Psychol Med 134:225–235.

Fuchs A, Kelso JAS, Haken H (1992) Phase transitions in the human brain: spatial mode dynamics. Int J Bifurcat Chaos 2:917–939.

Gerstein GL, Perkel DH (1969) Simultaneously recorded trains of action potentials: analysis and functional interpretation. Science 164:828–830.

Gerstein GL, Bedenbaugh P, Aertsen AM (1989) Neuronal assemblies. IEEE Trans Biomed Eng 36:4–14.

Gochin PM, Miller EK, Gross CG, Gerstein GL (1991) Functional interactions among neurons in inferior temporal cortex of the awake macaque. Exp Brain Res 84:505–516.

Goldenberg G (1989) The ability of patients with brain damage to generate mental visual images. Brain 112:305–325.

Goldenberg G, Podreka T, Suess E, Deecke L (1989) The cerebral localization of neuropsychological impairment in Alzheimer's disease: a SPECT study. J Neurol 236:131–138.

Goldman-Rakic PS (1986) Circuitry of primate prefrontal cortex and regulation of behavior by representational memory. In: Handbook of physiology, Vol 5 (Mountcastle VB, ed), pp 373–417. Baltimore: Williams and Wilkins.

Goldman-Rakic PS (1988) Topography of cognition: parallel distributed networks in primate association cortex. Annu Rev Neurosci 11:137–156.

Golub GH, Van Loan CF (1991) Matrix computations, 2d ed, pp 241–248. Baltimore: Johns Hopkins UP.

Gower JC (1966) Some distance properties of latent root and vector methods used in multivariate analysis. Biometrika 53:325–328.

Mayer-Kress G, Barczys C, Freeman W (1991) Attractor reconstruction from event-related multi-electrode EEG data. In: Mathematical approaches to brain functioning diagnostics (Dvorak I, Holden AV, eds). New York: Manchester UP.

McCarley RW, Shenton ME, O'Donnell BF, Faux SF, Kikinis R, Nestor PG, Jolesz FA (1993) Auditory P300 abnormalities and left posterior superior temporal gyrus volume reduction in schizophrenia. Arch Gen Psychiatry 50:190–197.

Newton I (1704) Opticks, Bk 1, Pt 2, Prop 6. London: Smith and Walford.

Shenton ME, Kikinis R, Jolesz FA, Pollak SD, Lemay M, Wible CG, Hokama H, Martin J, Metcalf D, Coleman M, McCarley RW (1992) Abnormalities of the left temporal lobe and thought disorder in schizophrenia—a quantitative magnetic resonance imaging study. N Engl J Med 327:604–612.

Shepard RN (1980) Multidimensional scaling, tree-fitting and clustering. Science 210:390–398.

Simmen MW, Goodhilll GJ, Willshaw DJ (1994) Scaling and brain connectivity. Nature 369:448–449.
Talairach J, Tournoux P (1988) A Co-planar stereotaxic atlas of a human brain. Stuttgart: Thieme.
Torgerson WS (1958) Theory and methods of scaling. New York: Wiley.
Weinberger DR (1987) Implications of normal brain development for the pathogenesis of schizophrenia. Arch Gen Psychiatry 44: 660–669.
Williamson P, Pelz D, Merskey H, Morrison S, Karlik S, Drost D, Carr T, Conlon P (1992) Frontal, temporal and striatal proton relaxation times in schizophrenic patients and normal comparison subjects. Am J Psychiatry 149:549–551.
Young MP (1992) Objective analysis of the topological organization of the primate cortical visual system. Nature 358:152–155.
Young MP, Scanell JW, Burns GAPC, Blakemore C (1994) Reply to Simmen et al. Nature 369:449–450.